Journal Pre-proof

BSA Fragmentation Specifically Induced by Added Electrolytes: an Electrospray Ionization Mass Spectrometry Investigation

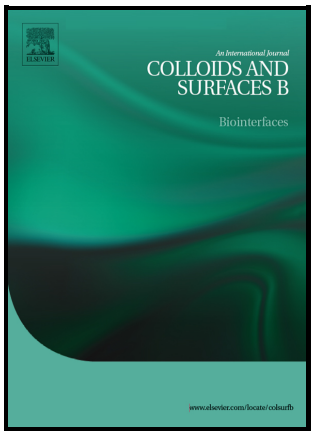

Gloria Lusci, Tiziana Pivetta, Cristina Carucci, Drew Francis Parsons, Andrea Salis, Maura Monduzzi

PII: S0927-7765(22)00409-X

DOI: https://doi.org/10.1016/j.colsurfb.2022.112726

Reference: COLSUB112726

To appear in: *Colloids and Surfaces B: Biointerfaces*

Received date: 24 March 2022
Revised date: 16 July 2022
Accepted date: 24 July 2022

Please cite this article as: Gloria Lusci, Tiziana Pivetta, Cristina Carucci, Drew Francis Parsons, Andrea Salis and Maura Monduzzi, BSA Fragmentation Specifically Induced by Added Electrolytes: an Electrospray Ionization Mass Spectrometry Investigation, *Colloids and Surfaces B: Biointerfaces,* (2022) doi:https://doi.org/10.1016/j.colsurfb.2022.112726

BSA Fragmentation Specifically Induced by Added Electrolytes: an Electrospray Ionization Mass Spectrometry Investigation

Gloria Lusci,[a] Tiziana Pivetta,[a] Cristina Carucci,[a,b] Drew Francis Parsons,* [a,b] Andrea Salis,* [a,b] and Maura Monduzzi * [a,b]

[a] Dept. Chemical and Geological Science, University of Cagliari, Cittadella Universitaria, S.S. 554 bivio Sestu, 09042 Monserrato, Cagliari, Italy;

[b] Consorzio Interuniversitario per lo Sviluppo dei Sistemi a Grande Interfase (CSGI), via della Lastruccia 3, 50019, Sesto Fiorentino (FI), Italy. Unità Operativa University of Cagliari, Cittadella Universitaria, SS 554 bivio Sestu, 09042 Monserrato (CA), Italy

***Corresponding authors:**
Maura Monduzzi: monduzzi@unica.it; ORCID 0000-0003-0200-7700
Drew F. Parsons: drew.parsons@unica.it ; ORCID 0000-0002-3956-6031
Andrea Salis: asalis@unica.it; ORCID 0000-0001-5746-2693

Abstract

Biointerfaces are significantly affected by electrolytes according to the Hofmeister series. This work reports a systematic investigation on the effect of different metal chlorides, sodium and potassium bromides, iodides and thiocyanates, on the ESI/MS spectra of bovine serum albumin (BSA) in aqueous solution at pH = 2.7. The concentration of each salt was varied to maximize the quality of the ESI/MS spectrum, in terms of peak intensity and bell-shaped profile. The ESI/MS spectra of BSA in the absence and in the presence of salts showed a main protein pattern characterized by the expected mass of 66.5 kDa, except the case of BSA/RbCl (mass 65,3 kDa). In all systems we observed an additional pattern, characterized by at least three peaks with low intensity, whose deconvolution led to suggest the formation of a BSA fragment with a mass of 19.2 kDa. Only NaCl increased the intensity of the peaks of the main BSA pattern, while minimizing that of the fragment. NaCl addition seems to play a crucial role in stabilizing BSA ionized interface against hydrolysis of peptide bonds, through different synergistic mechanisms. To quantify the

observed specific electrolyte effects, two “Hofmeister” parameters (*Hs* and *Ps*) are proposed. They are obtained using the ratio of (BSA-Salt)/BSA peak intensities for both the BSA main pattern and for its fragment.

Keywords: Bovine Serum Albumin, ESI/MS, BSA fragmentation, Specific electrolyte effects

Synopsis
NaCl stabilizes BSA ion and almost prevents fragmentation due to denaturing pH.

1. Introduction

The specific effect of cations and anions on the properties and on the behavior of proteins in solution has widely been investigated since Hofmeister's first observations.[1–6] Briefly, anions generally promote protein precipitation in the order $HPO_4^{2-} > SO_4^{2-} > F^- > Cl^- > Br^- > I^- > NO_3^- > ClO_4^- > SCN^-$, whereas cations tend to favor precipitation in the order $Cs^+ > NH_4^+ > Rb^+ > K^+ > Na^+ > Li^+ > Mg^{2+} > Ca^{2+}$. The general rule is that highly hydrated anions (kosmotropic) and weakly hydrated cations (chaotropic) favor protein precipitation. Bovine serum albumin (BSA) has often been chosen as model protein for many basic studies. This is due to the importance of plasma serum albumin in membrane interactions and metal binding [7,8] as well as the electrolyte and pH mediated formation of a protein corona around nanoparticles which in turn is addressed by the interplay among different intermolecular interactions.[9–11] In the last decade we found that monovalent anion binding occurs at the BSA surface, thus affecting the isoelectric point, in the increasing order $Cl^- < Br^- < NO_3^- < I^- < SCN^-$.[12,13] Adsorption of BSA to charged surfaces has clearly been related not only to the presence of specific electrolytes but also to the pH and the ionic strength.[9] Notably, anions were found to increase the self-diffusion coefficient of BSA in the order $F^- < Cl^- < Br^- < I^- < SCN^-$, whereas cations did not follow a monotonic Hofmeister series, with the increase of the interaction parameter of the diffusion coefficient, determined by DLS, following the order $Cs^+ < Li^+ < Na^+ < K^+ < Rb^+$.[14] Furthermore, it is worth citing that also buffers,

which are made of weak electrolytes, show significant specific effects even at the same nominal concentration and pH values.[15–17]

Electrospray ionization mass spectrometry (ESI/MS) techniques have become relatively fashionable for its potential in investigating nucleic acids and proteins or other molecules of biological interest, since Fenn's work in 1989.[18–25] For the theoretical background, the technical details and the possible analytical applications we refer to the existing literature,[26–29] particularly to several interesting papers on protein behavior published by the Konermann group.[30–35] Some main features and related equations of ESI/MS are briefly described below. Several papers report on BSA investigations through ESI/MS techniques [36–47] however, to the best of our knowledge, no systematic study of specific ion effects on BSA in denaturing conditions has been made.

In this work we report on an ESI/MS investigation performed on BSA, focussing not only on the specific ion effects due to the added electrolytes, but also on the role of a denaturing environment, namely an acidic pH = 2.7. In these conditions, BSA is below the isoelectric point (BSA pI ≈ 4.7)[12] and is positively charged. BSA structure is well known and its three domains have been fully characterized.[43] In addition, the occurrence of some weak peptide bonds that can easily undergo hydrolysis[48] or interact with metal ions,[49] is well documented. Remarkably, BSA in highly acidic medium, and depending on concentration, was found to undergo unfolding and partial refolding of its globular arrangement.[50] Here we investigate the effect of different metal-chlorides, along with sodium and potassium bromides, iodides and thiocyanate, added to BSA 19 μM solutions at pH = 2.7. The concentration of each salt is specifically adjusted to maximize the quality of the ESI/MS spectra, while keeping constant all other experimental conditions. The choice of the positive ion mode of ESI/MS spectra acquisition, and the acid pH = 2.7 ensures the occurrence of the typical bell-shaped ESI/MS profile of BSA, characterized by a large number of

peaks at specific *m/z* values. [40,41,47,51]

1.1 ESI/MS background

An electrospray ionization source generally allows for a soft ionization that produces multiple charged species without significant fragmentation of the proteins or destruction of the weak noncovalent associated conjugates. The ESI source produces highly charged aqueous droplets containing the protein that, before entering the MS device, tend to shrink due to solvent evaporation. This process increases the charge density at the droplet surface, thus Coulombic repulsion starts to counteract the cohesive intermolecular forces of water, namely the surface tension.[30] The shrinking process causes instability of the droplet, and can continue only until the number of elementary charges *e* reaches a value defined as the Rayleigh limit z_R, which is given by the equation:[52]

$$z_R = (8\pi/e)(\varepsilon_0\, \gamma\, R^3)^{0.5} \qquad (1)$$

where R is the droplet radius, ε_0 the vacuum permittivity, and γ the surface tension. The use of this relation for ESI technique is discussed by Fenn in his Noble Lecture.[53] Briefly, the value of z_R indicates that electrostatic repulsion has overcome surface tension forces (see also the discussion reported in a quite exhaustive review by Konerman [54]). Assuming the value of surface tension γ = 72 mN/m (pure water), eq (1) can be approximated, according to De La Mora, [55] to the following:

$$z_R \approx 0.078\, M^{0.5} \qquad (2)$$

where M is the molecular mass (Da) of the protein inside the droplet. Considering eq. 1, we may assume also that possible changes in surface tension due to the addition of electrolytes can almost be neglected when dealing with macromolecules and proteins having high molecular weight and also low salt concentrations. In general small ions quickly come out of the charged droplet through an ion evaporation model (**IEM**) mechanism, while proteins in aqueous medium may undergo

different ion release mechanisms, which always involve a liquid-gas phase transition.[31] Unfolded proteins may come out from the droplet upon solvent evaporation according to various pathways: i) through a charge residue model **(CRM)** if the droplet charge approaches the Rayleigh limit value z_R; ii) through a chain ejection model (**CEM**) if a Coulombic rebalancing between the droplet and the polypeptide protruding chain occurs; iii) through a collision induced dissociation (**CID**) mechanism if protein dissociation is caused by either too high energies or particular additives.[31,33,35]

Many parameters may affect the electrospray ionization process, particularly the addition of volatile compounds such as acetonitrile that generally enhances sensitivity,[20,21,27] and also the addition of buffers and strong electrolytes. Strong electrolytes indeed can either modify macroscopic parameters such as pH, ionic strength, viscosity or surface tension of the aqueous environment (see eq. 1), or promote specific interactions at a molecular level, that in turn may form salt adducts.[15,16,36,37]

An interesting parameter that can be obtained from the analysis of ESI/MS spectra is the average charge state distribution (CSD) Z_{av}, defined by the relation:[56]

$$Z_{av} = (\Sigma\, z_i \times I_i)/ (\Sigma I_i) \qquad (3)$$

where z_i and I_i are the charge and the associated intensity at each *m/z* value, respectively. The CSD parameter is strongly affected by the structure of the whole protein during the liquid-gas phase transition.[38,39,56–59] Several authors suggested interesting relations between CSD and molecular mass M [20,27,55] or solvent accessible surface area A_s,[56,57,60,61] through power laws with variable coefficients. Notably A_s data, successfully used to characterize the intrinsically disordered proteins,[56,57,60,61] can also be useful to give evidence of the conformational changes that may occur as a result of specific interactions between proteins and additives [62,63]. Indeed, conformational changes and unfolding or even dissociation may occur in our investigated

systems, already in the liquid phase, because of the presence of electrolytes and of the denaturing acid conditions. According to literature data [56,57,60–63] the A_s values can be obtained using the following equation: [62]

$$A_s = 4.84\ M^{0.76} \qquad (4)$$

where M is the molecular mass of the protein. It is worth citing that Eq. (4) has been validated by several authors and for a large number of proteins.[56,57,60–63] Interestingly, the Grandori group developed significant relations between Z_{av} and mass M, as well as between Z_{av} and A_s, enabling an evaluation of the state of the protein, in terms of folded or unfolded structure (see the Eq. S1, reported in SI).[57,61]

2. Materials and Methods

2.1 Chemicals

Bovine serum albumin (BSA) (98%) was purchased from Sigma-Aldrich (H7379) and used without further purification. Formic acid (85%), NaCl (98%), KCl (99.5%), KBr (99%), KI (99.5%), and CsCl (99.5%) were from Carlo Erba (Italy); LiCl (99%) was from Janssen; RbCl (99%) and NaI (99%) were from Sigma-Aldrich; NaBr (99%) was from Acros; $MgCl_2.6H_2O$ (98%) was Alfa-Aesar; Acetonitrile (99.9%), NaSCN (98%), KSCN (99%) and $CaCl_2$ (99.99%) were from Sigma Aldrich (Milan, Italy). milliQ double distilled water was used to prepare all samples.

2.2 Mass spectrometry

Mass spectra were recorded in positive ion mode on a triple quadrupole QqQ Varian 310-MS mass spectrometer using the Atmospheric-Pressure Electrospray Ionisation (ESI) technique in the *m/z* 50–2000 range. The experimental conditions were set up to reduce fragmentation reactions, in particular: needle voltage 5500 V, shield voltage 600 V, housing temperature 60 °C, drying gas

temperature 150 °C, nebulizer gas pressure 20 PSI, drying gas pressure 20 PSI, and detector voltage 1800 V. The sample solutions were infused directly into the ESI source using a programmable syringe pump at a flow rate of 1.50 mL/h. A dwell time of 14 s was chosen, and the spectra were accumulated for at least 30 min in order to increase the signal to noise ratio.

The mass spectrometer was calibrated daily with ESI Tuning Mix (Agilent Technologies) prior to the measurements. The final samples were analyzed in triplicate. All ions listed in this manuscript correspond to the monoisotopic masses.

2.3 Samples for ESI/MS experiments

The samples were prepared by weighing about 76 mg (± 0.1 mg) of BSA and adding small concentrations (mM) of metal chloride solutions (cations: Li^+, Na^+, K^+, Rb^+, Cs^+, Mg^{+2}, Ca^{+2}) or sodium and potassium salts (anions: Br^-, I^-, SCN^-). Then, the addition of H_2O and HCOOH 0.4 wt% up to a volume of 5 mL for each sample allowed final solutions to be obtained at pH = 2.7. A volume of 850 µL of these solutions was diluted with 150 µL of CH_3CN, thus obtaining a final volume of 1 mL to be analyzed by ESI/MS.

All examined samples contained BSA 1.9 x 10^{-5} M in mQ water, 0.4 wt% of HCOOH and 15.0 wt% of CH_3CN, at pH = 2.7. The protein concentration was selected to provide the highest quality of ESI/MS spectra with the used experimental conditions. Similarly, different salt concentrations were chosen to maximize the quality of the ESI/MS spectra, in terms of resolution, intensity and preservation of the bell-shape of thedistribution of peaks. ESI/MS spectra of BSA samples were always characterized by very high noise, therefore, to improve the analysis of theeffects of salts, in terms of intensity at each *m/z* value, a smoothing filter corresponding to *m/z* = 5 was applied to all BSA and BSA-salt ESI/MS spectra, using the mMass, the Open Source Mass Spectrometry Tool by Martin Strohalm et al. [64] (see original and smoothed ESI/MS spectra in SI, Figures SI_1). To ascertain the occurrence of BSA-salt adducts the free software program UniDec (version 5.0.3) was

also used.[65–67] The 'Smooth Nearby Points' and 'Suppress artifacts' functions were always applied whereas the intensity threshold was adjusted depending on the observed experimental intensity. Table 1 reports the deconvolution data (mass values, used threshold, and fitting parameters DScore and UniScore) obtained through Unidec, whereas all deconvolution spectra and fitting graphs from Unidec program are reported in SI_ Appendix A.

Table 1. Deconvolution data obtained through Unidec program, in the region *m/z* = 1000-2000

System	Calculated BSA mass	Intensity Threshold	DScore	UniScore
BSA	66450	0.025	8.81	8.81
BSA + LiCl	66440	0.2	1.9	1.56
BSA + NaCl	66450	0.025	8.76	8.76
BSA + KCl	66440	0.05	9.4	9.37
BSA + RbCl	65200	0.11	5.07	4.98
BSA + CsCl	66440	0.14	8.07	8.05
BSA + $MgCl_2$	66660	0.07	7.39	7.34
BSA + $CaCl_2$	66560	0.11	7.67	7.64
BSA + NaBr	66440	0.13	5.39	5.37
BSA + NaI	66580	0.25	0.93	0.3*
BSA + NaSCN	66560	0.22	6.99	6.95*
BSA + KBr	66590	0.14	5.06	4.95*
BSA + KI	66600	0.18	5.45	5.41*
BSA + KSCN	62610	0.34	5.63	5.57*

* high number of artifacts are detected.

However, depending on the range of *m/z* used, the UniDec program produced artifacts (see SI, Appendix A). Moreover Unidec did not allow identification of a fragment for which only 3-4 peaks in the correct sequence were observed (see next paragraph), due to the presence of too many weak peaks in the region *m/z* = 750-950 (see SI, Appendix A). Therefore for data treatment we used *m/z* values and peaks intensity obtained from the mMass program,[64] whereas to obtain z charges and mean masses we inserted *m/z* values in the ESIprot online program.[68] This approach was successfully used in a recent paper.[69] The list of the peaks used for deconvolution

is reported in SI, Tables SI_1. Notably, the masses for the BSA main profile calculated with both methods coincide except in the case of BSA+KSCN system, as shown in Table 2 below.

3. Results and discussion

3.1 ESI/MS data

The results of the ESI/MS experiments obtained for BSA in the absence and in the presence of the chosen salts, at different concentration, and at pH = 2.7, are presented here. Figure 1 shows the smoothed ESI/MS spectrum of BSA in the range *m/z* = 700-1900, along with the attribution of *z* charges obtained through the deconvolution procedure. The highest peak occurs at *m/z* = 1386.6, with a charge *z* = + 48. The deconvolution of the ESI spectra using the 9 peaks around the highest one allowed to calculate a mean molecular mass M = 66503 ± 9 Da for BSA. ESI/MS spectrum of BSA, at acidic pH, is very similar to those reported in other works[40–42,51] and the calculated molecular mass is very close to the usual value of 66.5 kDa reported for BSA.[42]

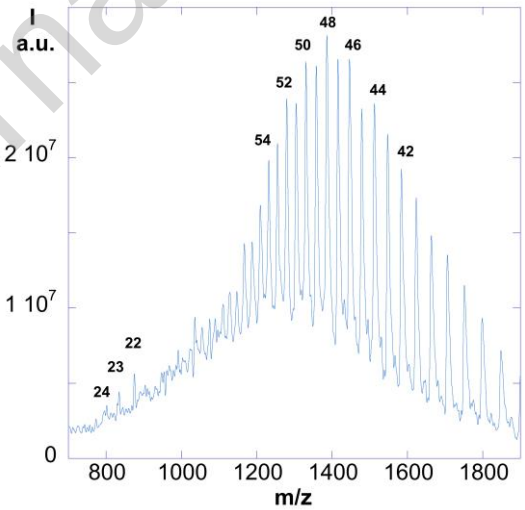

Figure 1. BSA ESI/MS smoothed (filter *m/z* = 5) spectrum in the range *m/z* = 700-1900 for BSA 1.9 x 10^{-5} M in H_2O containing HCOOH (0.4% w/w) and CH_3CN (15.0% w/w), pH = 2.7. **Intensity vs. *m/z*. Main pattern (mass 66.5 kDa):** in the range *m/z* ≈ 1200-1700 the attribution of z charges was obtained through deconvolution using the 9 peaks around the highest one. **Fragment (mass 19.2 kDa)** in the range *m/z* ≈ 750-950 the attribution of *z* charges was obtained through deconvolution using the 3 highest peaks (these 3 peaks appear also in the presence of salts at the same *m/z* values).

Remarkably, for BSA samples, particularly in the presence of several salts, an additional pattern constituted by at least 3 relatively weak peaks in the range *m/z* = 750-950 was observed (Figure 1). The deconvolution of these peaks, likely due to a BSA fragment, allowed to calculate the mass M = 19212 ± 35 Da, and to assign the positive charges *z* = 24, 23 and 22, for the BSA fragment pattern without salt.

The addition of salts induced important modifications in the intensity profile of the peaks of ESI/MS spectra, but in no case stable adducts formed by BSA protein were identified, likely because of the low salt/protein molar ratio. This is also confirmed by the Unidec program and can clearly be seen from the comparison between BSA in the absence and in the presence of salts made in two expanded regions of *m/z* values, shown in Figure 2 for some typical systems.

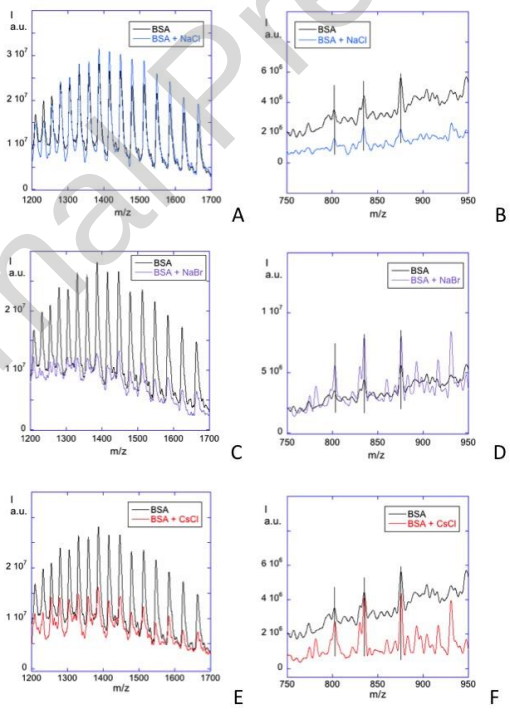

Figure 2. Expanded ESI/MS spectra in the range *m/z* = 1200-1700 (left side) and *m/z* = 750-950 (right side) for BSA compared to BSA + NaCl (A, B), BSA + NaBr (C,D) and BSA + CsCl (E,F) systems.

The absence of adducts can also be confirmed considering that no broadening of the bandwidth of the different peaks was observed (see Figure 2 and ref.[37,70]). On the other hand, the formation of protein-salt adducts may also be dependent on the ion source power. [71]

Table 2 summarizes the relevant features of the ESI/MS spectra of BSA in the presence of the various metal chlorides, and of sodium and potassium salts with the anions Br^-, I^-, and SCN^-, in the range *m/z* = 1200-1600. Table 3 summarizes the same relevant features for the fragment, in the range *m/z* = 750-950.

Table 2. BSA main protein pattern in the presence of different salts. Data from smoothed spectra. Concentration and Salt/BSA molar ratio. Highest Peak data: *m/z* values, Intensity I, *z* charges; Mean Mass (s.d. ≈ 0.6%) from deconvolution of the 9 peaks around the highest one, range *m/z* = 1200-1600; Quality of ESI/MS spectra.

BSA – Salt Sample	Conc. (mM)	Salt/BSA Molar ratio	*m/z*	I x 10^7 a.u.	Charge *z*	Mean Mass Da	*Quality ESI/MS
BSA no salt	0.019	-	1386.6	2.8	48	66503	high
LiCl	0.471	24.78	1385.4	1.4	48	66468	low
NaCl	0.163	8.58	1386.5	3.2	48	66504	high
KCl	0.196	10.31	1386.5	1.5	48	66514	high
RbCl	0.157	8.26	1362.7	0.65	48	65279	very low
CsCl	0.126	6.63	1386.9	1.5	48	66494	low
$MgCl_2$	0.320	16.84	1212.6	0.6	55	66649	low
$CaCl_2$	0.321	16.89	1331.5	1.1	48	66517	low
NaBr	0.162	8.53	1447.6	1.3	46	66495	very low
NaI	0.159	8.37	1386.1	0.98	48	66538	low
NaSCN	0.160	8.42	1386.1	0.98	48	66527	low
KBr	0.159	8.37	1388.8	1.3	48	66525	low
KI	0.163	8.58	1387.4	1.2	48	66543	low
KSCN	0.159	8.37	1330.9	0.5	50	66503	very low

*The notation 'very low' is used when both low intensity of the peaks and loss of bell-shaped profile are observed (See ESI/MS spectra in SI).

Table 3. BSA Fragment pattern in the presence of different salts. Data from smoothed spectra. Same samples and ESI/MS experiments as in Table 2. Highest Peak: *m/z* values, *z* charges; Mean Mass (s.d. ≈ 2%) from deconvolution of the 3 available peaks, range *m/z* = 750-950.

BSA – Salt Sample	h.p. *m/z*	I x 10^6 a.u.	h.p. *z*	Mean Mass Da
BSA no salt	875.6	5.6	22	19217
LiCl	835.1	4.8	23	19227
NaCl	834.8	2.4	23	19215
KCl	875.5	5.0	22	19220
RbCl	835.1	2.9	23	19223
CsCl	875.8	4.3	22	19225
$MgCl_2$	915.8	3.8	21	19213
$CaCl_2$	875.4	5.9	22	19209
NaBr	875.8	8.1	22	19223
NaI	875.8	7.2	22	19224
NaSCN	875.8	7.2	22	19224
KBr	835.0	7.5	23	19234
KI	875.9	7.5	22	19224
KSCN	875.8	5.0	22	19222

For BSA-salt systems the best spectra were obtained with salt concentration varying from a minimum value for CsCl (0.126 mM) to a maximum value for $CaCl_2$ (0.321 mM), as reported in the first column of Table 2. A BSA Salt/Protein molar ratio higher than 6 was always needed (second column in Table 2) to maximize the quality of ESI/MS spectra either in terms of intensity or shape profile. Interestingly the highest salt/protein molar ratio was found for LiCl (Li/BSA ≈ 24), and for $MgCl_2$ and $CaCl_2$ (Salt/BSA ≈ 16).

The quality of ESI/MS spectra is very good in the presence of NaCl, and KCl only, whereas the main BSA protein pattern is strongly affected by almost all the other salts. Clearly salt addition favors BSA fragmentation in highly acid aqueous solution before the liquid-gas transition.

A general observation can be made on the calculated mean mass values. BSA has MW = 66.5 kDa, and is constituted by 583 amino acids (a.a.) residues having a mean mass around 114 Da

Interestingly, for the BSA fragment pattern we obtained M ≈ 19.2 kDa (≈ 168 aa) for BSA either in the absence or in the presence of salts.

Summarizing the global effects produced by the various salts in regards to decreasing the quality of the BSA main protein profile and increasing the fragment intensity, we note that there is not theinverse relation that might otherwise be expected. For instance, CsCl addition produces a fragment with several intense peaks, but does not produce a very degraded spectrum of the BSA main protein pattern as shown in Figure 2E, and confirmed by Scores in Table 1 (see also spectra in SI and SI_Appendix A). The protein at pH = 2.7 has a highly positively charged exposed surface[50], and a significant anion interaction may be expected.[72,73] In addition we should not neglect that our anions in acidic medium may undergo a quick evaporation as A^- through an ion ejection model (IEM) mechanism associated with a decrease of surface tension.[74–76] Clearly BSA-anion electrostatic interactions and anion evaporation are competitive processes that, likely, can strongly be addressed by cation specific interactions with negatively charged or polarized a.a. residues at the BSA-water interface.

As for the fragment formation, BSA is known for its resistance to denaturation even at very low pH,[50] and often it undergoes reversible swelling phenomena caused by alterations in the weak interactions between the various secondary structures. It has been reported that there is a particularly weak bond between the a.a. 388-389, namely aspartic acid and proline, that can easily be hydrolyzed by heating in dilute formic acid.[48,49] The hydrolysis of this bond would generate two polypeptide fragments having masses around 44 and 22 kDa (in the crude approximation of an average a.a mass around 114 Da). It may tentatively be suggested that the fragment of 22 kDa in the very acidic environment undergoes further hydrolysis that produces a new stable fragment of about 19.2 kDa. Indeed, it is worth citing that serum albumins were found to undergo fragmentation within the thirty NH_2 terminal amino acids.[37] Actually, in other studies it has been

shown that hydrolysis processes of BSA peptide bonds can be favored by various electrolytes and metal complexes, as BSA has several sites sensitive to peptide bond breakdown.[41,48,49,77] Indeed, several variable fragments may form from BSA, as suggested by the crowd of peaks which appears in the presence of many salts, except NaCl and KCl, in the ESI/MS spectra in the region *m/z* = 750-1100 (see ESI/MS spectra in SI). Substantially, it may be suggested that the destiny of the droplets containing BSA in the presence of electrolytes is addressed by the interplay among ion induced weak or strong interactions, that causes either the ejection of the intact protein and its fragment (CEM mechanism) or the ejection of small ions (IEM mechanism). Notably, for all the investigated systems, we can rule out the CRM mechanism, not only because of the fragment formation, but also considering that z_R values of about 20 for the main BSA protein and of about 10 for the fragment, are calculated introducing the mean mass data reported in Tables 2 and 3 in eq. 2: the Rayleigh limit is not satisfied in any case. We can end this section highlighting the specific role of the ion pair NaCl in stabilizing highly charged BSA ion against fragmentation.

3.2 Electrolyte effects

To highlight and quantify salt effects, we can consider the ratio of (BSA-Salt)/BSA peak intensities at each *m/z* value. Figures 3A, and 3C report the (BSA-Salt)/BSA intensity ratio profile of the 9 peaks around the highest one observed for BSA-metal chloride systems, and for BSA in the presence of Na-X and K-X salts systems, respectively. Figures 3B, and 3D report a similar intensity ratio profile of the 3 peaks around the highest one observed for the fragment in BSA-Metal chlorides systems, and for BSA in the presence of Na-X and K-X salts systems, respectively.

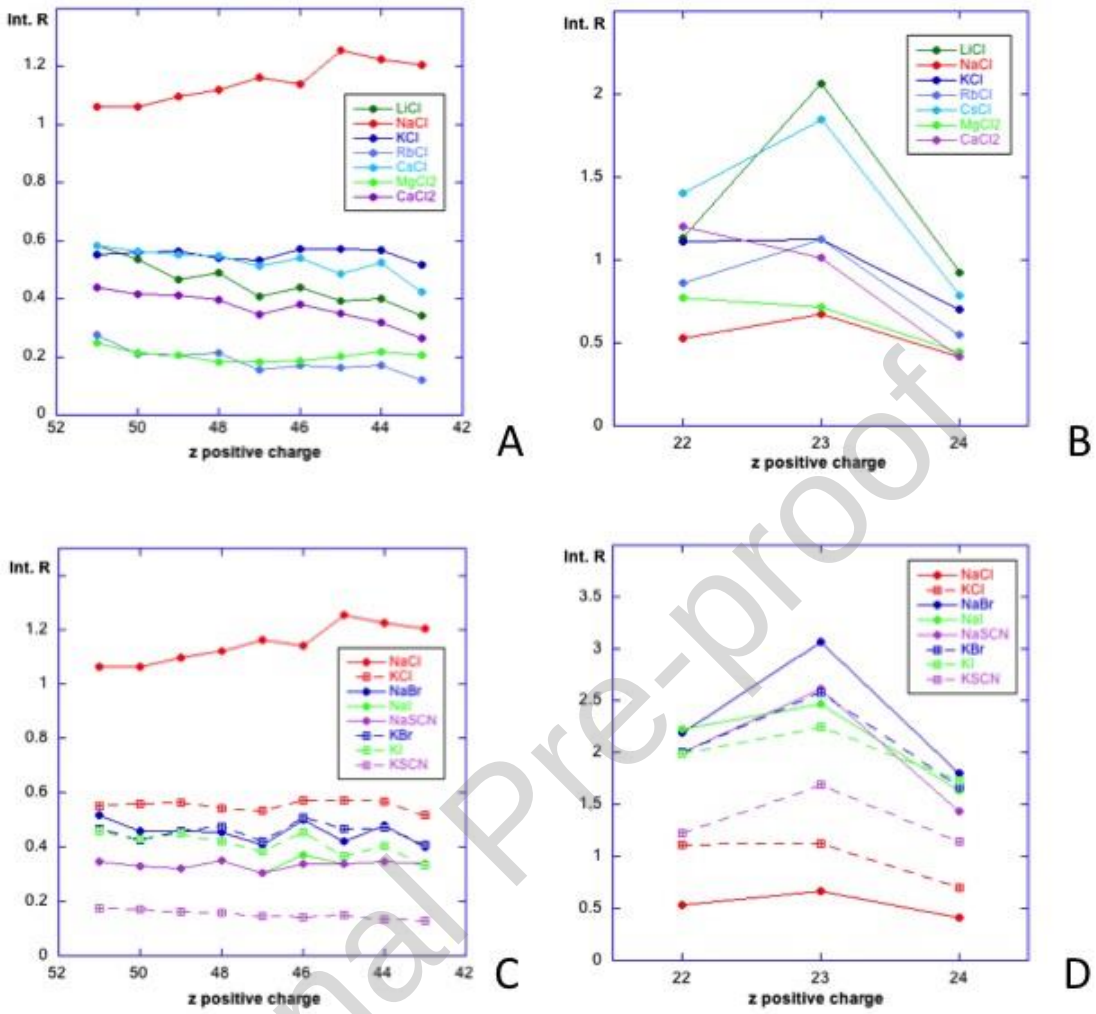

Figure 3. (**BSA-Salt)/BSA** peaks intensity ratio vs ***z*** positive charge: **A**) BSA-Metal chlorides main pattern; **B**) BSA-Metal chlorides fragment pattern; **C**) BSA main pattern in the presence of Na salts - continuous line – and K salt – dashed lines- with the anions Cl (red), Br (blue), I (green), SCN (violet); **D**) BSA fragment pattern in the presence of Na salts (continuous line), and K salts (dashed lines) with the anions Cl (red), Br (blue), I (green), SCN (violet).

Focusing on the profiles of Fig. 3A, to highlight cation effect at a qualitative level, we notice that the peaks' intensities and the quality of the ESI/MS spectra decrease in the order $Na^+ > K^+ \approx Cs^+ > Li^+ > Ca^{2+} > Rb^+ > Mg^{2+}$.

As for the effect of anions, the peaks intensity and the quality of the bell-shaped profile decrease in the order $Cl^- > Br^- > I^- > SCN^-$ for both Na^+ and K^+ salts as shown in Fig. 3C, in agreement with the Hofmeister series for anions. Interestingly, in the presence of NaCl, the intensity of all fragment

peaks is much lower than that found for BSA in the absence of salts as seen in Figure 2B (see also (BSA-Salt)/BSA intensity ratio in Figure 3B and 3D).

Indeed, the effect of cations in increasing the intensity of the fragment peaks (Fig. 3B) follows the decreasing order $Li^+ > Cs^+ > K^+ \approx Rb^+ > Ca^{2+} > Mg^{2+} > Na^+$. Considering the effect of the anions (Fig. 3D), the fragment formation is favored in the decreasing order by $Br^- > SCN^- \approx I^- > Cl^-$ for Na^+ salt (continuous lines), and by $Br^- > I^- > SCN^- > Cl^-$ for K^+ salts (dashed lines). Substantially, the fragment formation is favored particularly by Li^+ and Cs^+ cations and by Br^- anion, while as expected, very low fragmentation is observed with NaCl. Hence, we can suggest that NaCl promotes mainly the formation of a whole unfolded BSA charged ion, that implies a dominant CEM mechanism.

According to literature data [56,57,60–63] we checked for power law correlations between charge state distribution Z_{av} (eq.3), mass M (Table 2 and Table 3) and solvent accessible surface area A_s (eq. 4) (see SI Tables SI_2A and SI_2B where also the radius calculated from A_s values are reported), however no significant relations were found either between Z_{av} and M or between Z_{av} and A_s. Similar results were obtained also for the BSA fragment. This is not surprising since the limited range of molecular mass investigated in our systems likely prevents the possibility of obtaining correlations in agreement with literature equations which are, instead, based on a wide range of molecular mass. However, it is worth noting that the R values around 4.2 nm, calculated for BSA protein in the absence and in the presence of salts, are consistent with the hydrodynamic radius R_H = 4.5 (+0.2) nm obtained from the NMR self-diffusion coefficient $D_{BSA} = 4.56 \times 10^{-11}$ m^2 s^{-1} measured at 25 °C (see SI, note N1 for details).

3.3 Quantification of Hofmeister specific electrolytes effects

To quantify the salt effect, we can suggest two parameters that characterize the fluctuations of the (BSA-salt)/BSA intensity ratio at various z values in each system, as shown in Figure 3. We

define the average value of the peak intensity ratios H_S as the Hofmeister Specific Electrolyte parameter and define P_S, given by the relative variance (namely the ratio of the standard deviation of H_S to H_S), as the Specific Perturbation parameter. That is, H_S and P_S are defined bythe following relations:

$$H_S = \frac{1}{n}\sum_1^n I/I^\circ \qquad (5)$$

$$P_S = \frac{s.d.}{H_S} \qquad (6)$$

where *I/I°* is the (BSA-salt)/BSA intensity ratio of the peaks at each *z* value, and *n* is the number of peaks considered (see SI, Tables SI_3 and SI_4, for the ratios associated with each considered peak).

H_S represents the average specific electrolyte effect on the intensity profile of the ESI/MS peaks of BSA protein and of its fragment, both considered as a whole charged ion. The second parameter P_S highlights the significance of H_S being a measure of the structural loss in the charged protein ion ESI/MS profile, caused by specific electrolyte perturbations. Typically the lower the perturbation parameter P_S, the higher the Hofmeister electrolyte specificity H_S. Table 4 reports H_S parameter and its standard deviation, together with P_S parameter for both BSA main pattern and BSA fragment.

The Hofmeister contribution H_S allows to quantify the qualitative observations based on the quality of the ESI/MS spectra and on the trends of the intensity profiles reported in Fig. 3, referred to all the peaks in the different BSA systems.

Table 4. Hofmeister Specific Electrolyte parameter H_S and Specific Electrolyte Perturbation parameter P_S for BSA main pattern and BSA fragment.

Added salt	*BSA main pattern*			*BSA fragment*		
	H_S	H_S s.d.	P_S	H_S	H_S s.d.	P_S
LiCl	0.45	0.08	0.18	1.37	0.60	0.44
NaCl	1.15	0.07	0.01	0.54	0.13	0.24
KCl	0.55	0.02	0.04	0.98	0.24	0.24
RbCl	0.19	0.05	0.26	0.85	0.29	0.34
CsCl	0.53	0.05	0.09	1.35	0.53	0.39
$MgCl_2$	0.21	0.02	0.10	0.64	0.18	0.28
$CaCl_2$	0.37	0.06	0.16	0.88	0.41	0.47
NaBr	0.46	0.04	0.09	2.35	0.65	0.28
NaI	0.34	0.02	0.06	2.11	0.43	0.20
NaSCN	0.33	0.02	0.06	2.02	0.59	0.29
KBr	0.46	0.03	0.07	2.08	0.46	0.22
KI	0.41	0.04	0.10	1.99	0.25	0.13
KSCN	0.15	0.02	0.13	1.35	0.29	0.21

The combined effect of cations and anions on BSA profile and on the extent of salt-induced fragment formation can more clearly be seen in Fig. 4, where the H_S values are reported in the decreasing order of the added salts, for both the BSA main pattern (Fig. 4A) and fragment pattern (Fig. 4B), together with the associated perturbation parameter P_S that can provide the intrinsic significance of the specific electrolyte effect. Signficantly, both H_S and P_S values are always higher in the fragment pattern than in the intact protein ion profile.

Considering the effect of replacing chloride counterion with bromide, iodide, and thiocyanate for the Na^+ cation we can remark that the value $H_S > 1$ (lowest P_S) for NaCl compared to the $H_S << 1$, determined for NaBr, NaI and NaSCN, highlights the loss of the protein main profile while the intensity of fragment peaks increases. This, in turn, agrees with the $H_S > 2$ (low P_S) determined for BSA fragment in the presence of NaBr, NaI and NaSCN, and with the $H_S \approx 0.5$ obtained in the presence of NaCl.

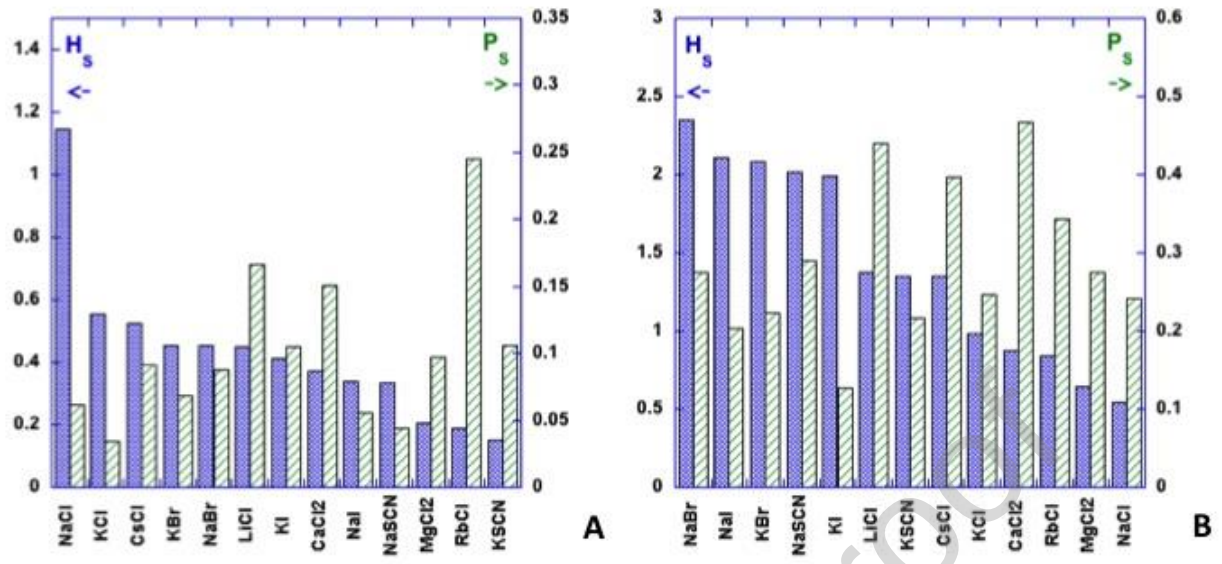

Figure 4. Hofmeister Electrolyte Specific Parameters H_S and P_S as a function of added electrolytes to BSA systems: A) Main pattern; B) Fragment pattern.

Notably, the H_S values, referred to BSA main protein pattern show the anion decreasing sequence $Cl^- > Br^- > I^- > SCN^-$, while for fragment formation, the anion decreasing sequence becomes $Br^- > I^- > SCN^- > Cl^-$ for both Na and K salts. Substantially, chloride anion favors hydrolysis driven fragmentation at a much lower extent than bromide anion, but, in turn, promotes high perturbations of the structure, as suggested by low H_S and high P_S values in Fig. 4A for BSA main pattern, particularly when associated to Li^+, Rb^+, Mg^{2+} and Ca^{2+} cations.

As to the Hofmeister Specific Electrolyte parameters H_S and P_S shown in Fig. 4, we can remark the following points: i) only in the case of NaCl addition the H_S value confirms the opposite behavior, qualitatively observed, that is enhancing the main BSA pattern and minimizing fragment formation; ii) all the other electrolytes produce different effects for BSA main and fragment pattern; iii) NaBr, NaI, KBr, NaSCN, and also KI with $H_S \geq 2$, show a specific propensity in favoring fragment formation, without, however, destroying the BSA main pattern; iv) Br^- anion causes the highest fragmentation of BSA protein in both BSA-NaX and BSA-KX systems (notably NaBr > KBr).

The effect of NaCl is not easy to understand, however we can suggest that NaCl specifically modifies the stability and the dynamic behavior of unfolded BSA interface thus preventing the breaking of some weak peptide bonds that was observed for the other salts.[48,49] To the best of our knowledge, no data on NaCl stabilizing effects towards BSA in pH-induced denaturing conditions are available. Nevertheless, we can consider some works where the thermally induced BSA unfolding, at pH ≈ 7, produces aggregation and then induces a sol-gel transition due to crosslinking, as demonstrated through various techniques.[78,79] Indeed the sol-gel transition was found to depend on the BSA critical concentration that decreased with increasing NaCl concentration.[78] In addition, the presence of NaCl was suggested to retard the kinetics of the post-denaturation fragmentation phenomena thus allowing for a re-compaction of the domains upon cooling.[79] On the other hand, we should mention that BSA unfolding induced by heating was ascertained to produce structural modifications involving also the melting of α-helices that facilitates gelling processes as found for a solution of BSA containing NaCl.[80,81]

4. Concluding remarks

This work clearly shows that salts affect specifically the ESI/MS spectra of BSA protein, in denaturing solution, in a more complicated manner than the conventional Hofmeister series, likely due to different interactions and fragmentations which occur in the liquid state. Among the observed results, one of the most interesting is certainly related to the formation of a BSA fragment with a mass of about 19.2 kDa, due to acidic hydrolysis at some weak peptide bonds (aspartic acid is particularly prone to undergo acid induced hydrolysis), and dependent on the type of added salt. BSA undergoes fragmentation either in the absence or in the presence of salts, and the liquid-gas transition of BSA and its fragment occurs through the CEM mechanism, that is a chain ejection model after ion-mediated charge rebalance. Moreover, since the pH is lower than the BSA pI, in principle we might expect a substantial effect due to anion binding that, however, is

a process in competition with ion ejection as A^-. Due to the very low concentration of added salts, the replacement of H^+ with other cations does not seem to be particularly favored, nevertheless cations clearly play a significant role in addressing the fate of BSA ion and its fragment.

The proposed H_S parameter mainly represents the quantification of the added salt effects rather than the usual anion or cation trend within the Hofmeister series framework.

We conclude by highlighting the unique specificity of NaCl in stabilizing the BSA ion and enhancing BSA peak intensities in the ESI/MS spectrum, and also the dramatic effect of replacing Cl^- anion with Br^-, I^-, and SCN^- anion in the Na^+ and K^+ salts systems, for which, remarkably, very similar concentrations, in terms of molar ratio, were used.

Acknowledgements

Financial supports from FIR 2020, Fondazione di Sardegna (FdS, F72F20000230007), and Regione Sardegna L.R. 7 (CUP: J81G17000150002 and CRP: RASSR79857) are gratefully acknowledged. Prof. Enrico Sanjust is ackowledged for his kind and useful suggestions. C.C. thanks MIUR (PON-AIM Azione I.2, DD 407- 27.02.2018, AIM1890410-2) for funding. CeSAR (Centro Servizi di Ateneo per la Ricerca) of the University of Cagliari is acknowledged for the use of NMR facilities. Dr. Sandrina Lampis is thanked for her essential technical support.

References

[1] F. Hofmeister, Zur Lehre von der Wirkung der Salze, Arch. Für Exp. Pathol. Und Pharmakologie. 24 (1888) 247–260. doi:10.1007/BF01918191.

[2] W. Kunz, J. Henle, B.W. Ninham, "Zur Lehre von der Wirkung der Salze" (about the science of the effect of salts): Franz Hofmeister's historical papers, Curr. Opin. Colloid Interface Sci. 9 (2004) 19–37. doi:10.1016/j.cocis.2004.05.005.

[3] P. Lo Nostro, B.W. Ninham, Hofmeister Phenomena: An Update on Ion Specificity in Biology, Chem. Rev. 112 (2012) 2286–2322. doi:10.1021/cr200271j.

[4] A. Salis, B.W. Ninham, Models and mechanisms of Hofmeister effects in electrolyte solutions, and colloid and protein systems revisited, Chem. Soc. Rev. 43 (2014) 7358–7377. doi:10.1039/c4cs00144c.

[5] P. Lo Nostro, B.W. Ninham, Editorial: Electrolytes and specific ion effects. New and old horizons, Curr. Opin. Colloid Interface Sci. 23 (2016) A1–A5. doi:10.1016/j.cocis.2016.06.007.

[6] M.A. Budroni, F. Rossi, N. Marchettini, F. Wodlei, P. Lo Nostro, M. Rustici, Hofmeister Effect in Self-Organized Chemical Systems, J. Phys. Chem. B. 124 (2020) 9658–9667. doi:10.1021/acs.jpcb.0c06956.

[7] K.A. Majorek, P.J. Porebski, A. Dayal, M.D. Zimmerman, K. Jablonska, A.J. Stewart, M. Chruszcz, W. Minor, Structural and immunologic characterization of bovine, horse, and rabbit serum albumins, Mol. Immunol. 52 (2012) 174–182. doi:10.1016/j.molimm.2012.05.011.

[8] F. Sebastiani, M. Yanez Arteta, L. Lindfors, M. Cárdenas, Screening of the binding affinity of serum proteins to lipid nanoparticles in a cell free environment, J. Colloid Interface Sci. 610 (2022) 766–774. doi:10.1016/j.jcis.2021.11.117.

[9] A. Salis, L. Medda, F. Cugia, M. Monduzzi, Effect of electrolytes on proteins physisorption on ordered mesoporous silica materials, Colloids Surfaces B Biointerfaces. 137 (2016) 77–90. doi:10.1016/j.colsurfb.2015.04.068.

[10] V. Nairi, S. Medda, M. Piludu, M.F. Casula, M. Vallet-Regì, M. Monduzzi, A. Salis, Interactions between bovine serum albumin and mesoporous silica nanoparticles functionalized with biopolymers, Chem. Eng. J. 340 (2018) 42–50. doi:10.1016/j.cej.2018.01.011.

[11] G.R. Delpiano, M.F. Casula, M. Piludu, R. Corpino, P.C. Ricci, M. Vallet-Regí, E. Sanjust, M. Monduzzi, A. Salis, Assembly of Multicomponent Nano-Bioconjugates Composed of Mesoporous Silica Nanoparticles, Proteins, and Gold Nanoparticles, ACS Omega. 4 (2019) 11044–11052. doi:10.1021/acsomega.9b01240.

[12] A. Salis, M. Boström, L. Medda, F. Cugia, B. Barse, D.F. Parsons, B.W. Ninham, M. Monduzzi, Measurements and Theoretical Interpretation of Points of Zero Charge/Potential of BSA Protein, Langmuir. 27 (2011) 11597–11604. doi:10.1021/la2024605.

[13] L. Medda, B. Barse, F. Cugia, M. Boström, D.F. Parsons, B.W. Ninham, M. Monduzzi, A. Salis, Hofmeister Challenges: Ion Binding and Charge of the BSA Protein as Explicit Examples, Langmuir. 28 (2012) 16355–16363. doi:10.1021/la3035984.

[14] L. Medda, M. Monduzzi, A. Salis, The molecular motion of bovine serum albumin under physiological conditions is ion specific, Chem. Commun. 51 (2015) 6663–6666. doi:10.1039/C5CC01538C.

[15] A. Salis, M. Monduzzi, Not only pH. Specific buffer effects in biological systems, Curr. Opin. Colloid Interface Sci. 23 (2016) 1–9. doi:10.1016/j.cocis.2016.04.004.

[16] A. Salis, L. Cappai, C. Carucci, D.F. Parsons, M. Monduzzi, Specific Buffer Effects on the Intermolecular Interactions among Protein Molecules at Physiological pH, J. Phys. Chem. Lett. 11 (2020) 6805–6811. doi:10.1021/acs.jpclett.0c01900.

[17] D.F. Parsons, A. Salis, Hofmeister effects at low salt concentration due to surface charge transfer, Curr. Opin. Colloid Interface Sci. 23 (2016) 41–49. doi:10.1016/j.cocis.2016.05.005.

[18] S.F. Wong, C.K. Meng, J.B. Fenn, Multiple charging in electrospray ionization of poly(ethylene glycols), J. Phys. Chem. 92 (1988) 546–550. doi:10.1021/j100313a058.

[19] J. Fenn, M. Mann, C. Meng, S. Wong, C. Whitehouse, Electrospray ionization for mass spectrometry of large biomolecules, Science (80-.). 246 (1989) 64–71. doi:10.1126/science.2675315.

[20] S. Banerjee, S. Mazumdar, Electrospray Ionization Mass Spectrometry: A Technique to Access the Information beyond the Molecular Weight of the Analyte, Int. J. Anal. Chem. 2012 (2012) 1–40. doi:10.1155/2012/282574.

[21] M. Przybylski, M.O. Glocker, Electrospray Mass Spectrometry of Biomacromolecular Complexes with Noncovalent Interactions—New Analytical Perspectives for Supramolecular Chemistry and Molecular Recognition Processes, Angew. Chemie Int. Ed. English. 35 (1996) 806–826. doi:10.1002/anie.199608061.

[22] D. Sanna, V. Ugone, G. Micera, T. Pivetta, E. Valletta, E. Garribba, Speciation of the Potential Antitumor Agent Vanadocene Dichloride in the Blood Plasma and Model Systems, Inorg. Chem. 54 (2015) 8237–8250. doi:10.1021/acs.inorgchem.5b01277.

[23] E. Cadoni, P. Vanhara, E. Valletta, E. Pinna, S. Vascellari, G. Caddeo, F. Isaia, A. Pani, J. Havel, T. Pivetta, Mass spectrometric discrimination of phospholipid patterns in cisplatin-resistant and -sensitive cancer cells, Rapid Commun. Mass Spectrom. 33 (2019) 97–106. doi:10.1002/rcm.8320.

[24] E. Cadoni, E. Valletta, G. Caddeo, F. Isaia, M.G. Cabiddu, S. Vascellari, T. Pivetta, Competitive reactions among glutathione, cisplatin and copper-phenanthroline complexes, J. Inorg. Biochem. 173 (2017) 126–133. doi:10.1016/j.jinorgbio.2017.05.004.

[25] S. Masuri, E. Cadoni, M.G. Cabiddu, F. Isaia, M.G. Demuru, L. Moráň, D. Buček, P. Vaňhara, J. Havel, T. Pivetta, The first copper(<scp>ii</scp>) complex with 1,10-phenanthroline and salubrinal with interesting biochemical properties, Metallomics. 12 (2020) 891–901. doi:10.1039/D0MT00006J.

[26] A.J.R. Heck, R.H.H. Van Den Heuvel, Investigation of intact protein complexes by mass spectrometry, Mass Spectrom. Rev. 23 (2004) 368–389. doi:10.1002/mas.10081.

[27] P. Kebarle, A brief overview of the present status of the mechanisms involved in electrospray mass spectrometry, J. Mass Spectrom. 35 (2000) 804–817. doi:10.1002/1096-9888(200007)35:7<804::AID-JMS22>3.0.CO;2-Q.

[28] U.H. Verkerk, P. Kebarle, Ion-ion and ion-molecule reactions at the surface of proteins produced by nanospray. Information on the number of acidic residues and control of the number of ionized acidic and basic residues, J. Am. Soc. Mass Spectrom. 16 (2005) 1325–1341. doi:10.1016/j.jasms.2005.03.018.

[29] B. V. Nielsen, D.A. Abaye, Influence of electrolytes and a supercharging reagent on charge

state distribution and response of neuropeptide ions generated during positive electrospray ionisation mass spectrometry, Eur. J. Mass Spectrom. 19 (2013) 335–344. doi:10.1255/ejms.1246.

[30] M.C. Kuprowski, B.L. Boys, L. Konermann, Analysis of Protein Mixtures by Electrospray Mass Spectrometry: Effects of Conformation and Desolvation Behavior on the Signal Intensities of Hemoglobin Subunits, J. Am. Soc. Mass Spectrom. 18 (2007) 1279–1285. doi:10.1016/j.jasms.2007.04.002.

[31] L. Konermann, E. Ahadi, A.D. Rodriguez, S. Vahidi, Unraveling the mechanism of electrospray ionization, Anal. Chem. 85 (2013) 2–9. doi:10.1021/ac302789c.

[32] J.J. Liu, L. Konermann, Cation-induced stabilization of protein complexes in the gas phase: Mechanistic insights from hemoglobin dissociation studies, J. Am. Soc. Mass Spectrom. 25 (2014) 595–603. doi:10.1007/s13361-013-0814-7.

[33] X. Yue, S. Vahidi, L. Konermann, Insights into the mechanism of protein electrospray ionization from salt adduction measurements, J. Am. Soc. Mass Spectrom. 25 (2014) 1322–1331. doi:10.1007/s13361-014-0905-0.

[34] L. Konermann, H. Metwally, Q. Duez, I. Peters, Charging and supercharging of proteins for mass spectrometry: Recent insights into the mechanisms of electrospray ionization, Analyst. 144 (2019) 6157–6171. doi:10.1039/c9an01201j.

[35] L.M. Martin, L. Konermann, Enhancing protein electrospray charge states by multivalent metal ions: Mechanistic insights from MD simulations and mass spectrometry experiments, J. Am. Soc. Mass Spectrom. 31 (2020) 25–33. doi:10.1021/jasms.9b00027.

[36] J.A. Loo, C.G. Edmonds, H.R. Udseth, R.D. Smith, Effect of reducing disulfide-containing proteins on electrospray ionization mass spectra, Anal. Chem. 62 (1990) 693–698. doi:10.1021/ac00206a009.

[37] J.A. Loo, C.G. Edmonds, R.D. Smith, Tandem mass spectrometry of very large molecules. 2. Dissociation of multiply charged proline-containing proteins from electrospray ionization, Anal. Chem. 65 (1993) 425–438. doi:10.1021/ac00052a020.

[38] Y. Zhong, L. Han, B.T. Ruotolo, Collisional and Coulombic Unfolding of Gas-Phase Proteins: High Correlation to Their Domain Structures in Solution, Angew. Chemie. 126 (2014) 9363–9366. doi:10.1002/ange.201403784.

[39] J.D. Eschweiler, R.M. Martini, B.T. Ruotolo, Chemical Probes and Engineered Constructs Reveal a Detailed Unfolding Mechanism for a Solvent-Free Multidomain Protein, J. Am. Chem. Soc. 139 (2017) 534–540. doi:10.1021/jacs.6b11678.

[40] R. Bakhtiar, F.L.S. Tse, Biological mass spectrometry: A primer, Mutagenesis. 15 (2000) 415–430. doi:10.1093/mutage/15.5.415.

[41] E. Da Silva, C.F. Rousseau, I. Zanella-Cléon, M. Becchi, A.W. Coleman, Mass Spectrometric Determination of Association Constants of Bovine Serum Albumin (BSA) with para-Sulphonato-Calix[n]arene Derivatives, J. Incl. Phenom. Macrocycl. Chem. 54 (2006) 53–59. doi:10.1007/s10847-005-3995-2.

[42] K. Hirayama, S. Akashi, M. Furuya, K. Fukuhara, Rapid Confirmation and Revision of the Primary Structure of Bovine Serum Albumin by ESIMS and FRIT-FAB LC/MS., Biochem. Biophys. Res. Commun. 173 (1990) 639–646.

[43] I. Rombouts, B. Lagrain, K.A. Scherf, M.A. Lambrecht, P. Koehler, J.A. Delcour, Formation

and reshuffling of disulfide bonds in bovine serum albumin demonstrated using tandem mass spectrometry with collision-induced and electron-transfer dissociation, Sci. Rep. 5 (2015) 12210. doi:10.1038/srep12210.

[44] M.T. Donor, S.A. Ewing, M.A. Zenaidee, W.A. Donald, J.S. Prell, Extended Protein Ions Are Formed by the Chain Ejection Model in Chemical Supercharging Electrospray Ionization, Anal. Chem. 89 (2017) 5107–5114. doi:10.1021/acs.analchem.7b00673.

[45] E.D.B. Foley, M.A. Zenaidee, R.F. Tabor, J. Ho, J.E. Beves, W.A. Donald, On the mechanism of protein supercharging in electrospray ionisation mass spectrometry: Effects on charging of additives with short- and long-chain alkyl constituents with carbonate and sulphite terminal groups, Anal. Chim. Acta X. 1 (2019) 100004. doi:10.1016/j.acax.2018.100004.

[46] G. Chen, M. Fan, Y. Liu, B. Sun, M. Liu, J. Wu, N. Li, M. Guo, Advances in MS Based Strategies for Probing Ligand-Target Interactions: Focus on Soft Ionization Mass Spectrometric Techniques, Front. Chem. 7 (2019) 1–17. doi:10.3389/fchem.2019.00703.

[47] B.X. Huang, H. Kim, C. Dass, Probing Three-Dimensional Structure of Bovine Serum Albumin by Chemical Cross-Linking and Mass Spectrometry, J Am Soc Mass Spectrom. 15 (2004) 1237–1247. doi:10.1016/j.jasms.2004.05.004.

[48] G. Weber, L.B. Young, Fragmentation of Bovine Serum Albumin by Pepsin, J. Biol. Chem. 239 (1964) 1415–1423. doi:10.1016/S0021-9258(18)91331-1.

[49] N.E. Wezynfeld, T. Frączyk, W. Bal, Metal assisted peptide bond hydrolysis: Chemistry, biotechnology and toxicological implications, Coord. Chem. Rev. 327–328 (2016) 166–187. doi:10.1016/j.ccr.2016.02.009.

[50] L.R.S. Barbosa, M.G. Ortore, F. Spinozzi, P. Mariani, S. Bernstorff, R. Itri, The importance of protein-protein interactions on the pH-induced conformational changes of bovine serum albumin: A small-angle x-ray scattering study, Biophys. J. 98 (2010) 147–157. doi:10.1016/j.bpj.2009.09.056.

[51] M.A. Zenaidee, W.A. Donald, Electron capture dissociation of extremely supercharged protein ions formed by electrospray ionisation, Anal. Methods. 7 (2015) 7132–7139. doi:10.1039/c5ay00710k.

[52] L. Rayleigh, No Title, Philos. Mag. 14 (1882) 184.

[53] J.B. Fenn, Electrospray Wings for Molecular Elephants (Nobel Lecture), Angew. Chemie Int. Ed. 42 (2003) 3871–3894. doi:10.1002/anie.200300605.

[54] L. Konermann, A simple model for the disintegration of highly charged solvent droplets during electrospray ionization, J. Am. Soc. Mass Spectrom. 20 (2009) 496–506. doi:10.1016/j.jasms.2008.11.007.

[55] J. Fernandez De La Mora, Electrospray ionization of large multiply charged species proceeds via Dole's charged residue mechanism, Anal. Chim. Acta. 406 (2000) 93–104. doi:10.1016/S0003-2670(99)00601-7.

[56] J. Li, C. Santambrogio, S. Brocca, G. Rossetti, P. Carloni, R. Grandori, Conformational effects in protein electrospray-ionization mass spectrometry, Mass Spectrom. Rev. 35 (2016) 111–122. doi:10.1002/mas.21465.

[57] A. Natalello, C. Santambrogio, R. Grandori, Are Charge-State Distributions a Reliable Tool Describing Molecular Ensembles of Intrinsically Disordered Proteins by Native MS?, J. Am. Soc. Mass Spectrom. 28 (2017) 21–28. doi:10.1007/s13361-016-1490-1.

[58] Z. Hall, C. V. Robinson, Do charge state signatures guarantee protein conformations?, J. Am. Soc. Mass Spectrom. 23 (2012) 1161–1168. doi:10.1007/s13361-012-0393-z.

[59] I.A. Kaltashov, A. Mohimen, Estimates of protein surface areas in solution by electrospray ionization mass spectrometry, Anal. Chem. 77 (2005) 5370–5379. doi:10.1021/ac050511+.

[60] M. Šamalikova, R. Grandori, Protein Charge-State Distributions in Electrospray-Ionization Mass Spectrometry Do Not Appear to Be Limited by the Surface Tension of the Solvent, J. Am. Chem. Soc. 125 (2003) 13352–13353. doi:10.1021/ja037000u.

[61] L. Testa, S. Brocca, R. Grandori, Charge-surface correlation in electrospray ionization of folded and unfolded proteins, Anal. Chem. 83 (2011) 6459–6463. doi:10.1021/ac201740z.

[62] J.A. Marsh, S.A. Teichmann, Relative solvent accessible surface area predicts protein conformational changes upon binding, Structure. 19 (2011) 859–867. doi:10.1016/j.str.2011.03.010.

[63] J.A. Marsh, Buried and accessible surface area control intrinsic protein flexibility, J. Mol. Biol. 425 (2013) 3250–3263. doi:10.1016/j.jmb.2013.06.019.

[64] M. Strohalm, D. Kavan, P. Novák, M. Volný, V. Havlíček, mMass 3: A Cross-Platform Software Environment for Precise Analysis of Mass Spectrometric Data, Anal. Chem. 82 (2010) 4648–4651. doi:10.1021/ac100818g.

[65] M.T. Marty, A.J. Baldwin, E.G. Marklund, G.K.A. Hochberg, J.L.P. Benesch, C. V. Robinson, Bayesian Deconvolution of Mass and Ion Mobility Spectra: From Binary Interactions to Polydisperse Ensembles, Anal. Chem. 87 (2015) 4370–4376. doi:10.1021/acs.analchem.5b00140.

[66] M.T. Marty, Eliminating Artifacts in Electrospray Deconvolution with a SoftMax Function, J. Am. Soc. Mass Spectrom. 30 (2019) 2174–2177. doi:10.1007/s13361-019-02286-4.

[67] M.T. Marty, A Universal Score for Deconvolution of Intact Protein and Native Electrospray Mass Spectra, Anal. Chem. 92 (2020) 4395–4401. doi:10.1021/acs.analchem.9b05272.

[68] R. Winkler, ESIprot: a universal tool for charge state determination and molecular weight calculation of proteins from electrospray ionization mass spectrometry data, Rapid Commun. Mass Spectrom. 24 (2010) 285–294. doi:10.1002/rcm.4384.

[69] T. Pivetta, G. Lusci, C. Carucci, D.F. Parsons, A. Salis, M. Monduzzi, Specific electrolyte effects on hemoglobin in denaturing medium investigated through electro spray ionization mass spectrometry, J. Inorg. Biochem. 234 (2022) 111872. doi:10.1016/j.jinorgbio.2022.111872.

[70] D.J. Clarke, D.J. Campopiano, Desalting large protein complexes during native electrospray mass spectrometry by addition of amino acids to the working solution, Analyst. 140 (2015) 2679–2686. doi:10.1039/C4AN02334J.

[71] R. Juraschek, T. Dulcks, M. Karas, Nanoelectrospray — More Than Just a Minimized-Flow Electrospray Ionization Source, J Am Soc Mass Spectrom. 10 (1999) 300–308.

[72] C. Tanford, S.A. Swanson, W.S. Shore, Hydrogen Ion Equilibria of Bovine Serum Albumin 1, J. Am. Chem. Soc. 77 (1955) 6414–6421. doi:10.1021/ja01629a002.

[73] C. Tanford, J.G. Buzzell, D.G. Rands, S.A. Swanson, The Sedimentation Behavior of Bovine Serum Albumin in Acid Solutions 1, J. Am. Chem. Soc. 77 (1955) 6421–6428.

[74] Y. Marcus, Surface Tension of Aqueous Electrolytes and Ions, J. Chem. Eng. Data. 55 (2010) 3641–3644. doi:10.1021/je1002175.

[75] Y. Marcus, Specific ion effects on the surface tension and surface potential of aqueous electrolytes, Curr. Opin. Colloid Interface Sci. 23 (2016) 94–99. doi:10.1016/j.cocis.2016.06.016.

[76] Y. Marcus, A relationship between the effect of uni-univalent electrolytes on the structure of water and on its volatility, J. Chem. Phys. 148 (2018). doi:10.1063/1.5009311.

[77] N. V Goncharov, D.A. Belinskaia, V.I. Shmurak, M.A. Terpilowski, R.O. Jenkins, P. V Avdonin, Serum Albumin Binding and Esterase Activity: Mechanistic Interactions with Organophosphates, Molecules. 22 (2017) 1201. doi:10.3390/molecules22071201.

[78] L. Donato, C. Garnier, J.-L. Doublier, T. Nicolai, Influence of the NaCl or CaCl 2 Concentration on the Structure of Heat-Set Bovine Serum Albumin Gels at pH 7, Biomacromolecules. 6 (2005) 2157–2163. doi:10.1021/bm050132q.

[79] O. Matsarskaia, L. Bühl, C. Beck, M. Grimaldo, R. Schweins, F. Zhang, T. Seydel, F. Schreiber, F. Roosen-Runge, Evolution of the structure and dynamics of bovine serum albumin induced by thermal denaturation, Phys. Chem. Chem. Phys. 22 (2020) 18507–18517. doi:10.1039/D0CP01857K.

[80] M. Yamasaki, H. Yano, K. Aoki, Differential scanning calorimetric studies on bovine serum albumin: I. Effects of pH and ionic strength, Int. J. Biol. Macromol. 12 (1990) 263–268. doi:10.1016/0141-8130(90)90007-W.

[81] K. Murayama, M. Tomida, Heat-Induced Secondary Structure and Conformation Change of Bovine Serum Albumin Investigated by Fourier Transform Infrared Spectroscopy, Biochemistry. 43 (2004) 11526–11532. doi:10.1021/bi0489154.

Graphical abstract

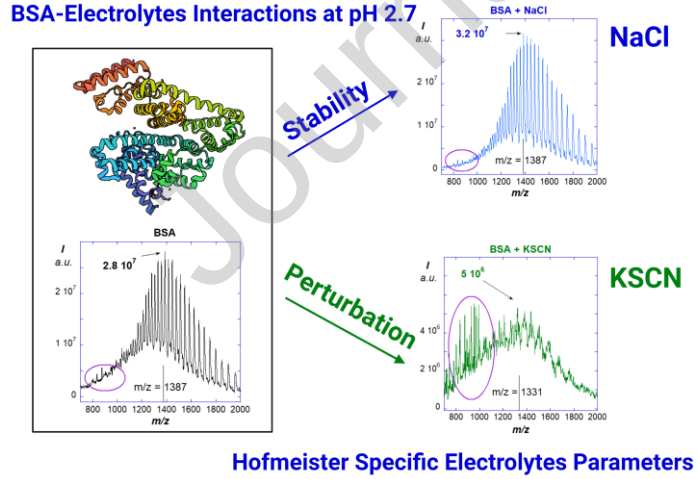

CRediT authorship contribution statement

Gloria Lusci: Data curation and Investigation.

Tiziana Pivetta: Data curation and Investigation (lead); Resources and Supervision (equal); Project administration.

Cristina Carucci: Visualization.

Drew F. Parsons: Formal analysis and Validation; Writing-Review &Editing (equal);

Andrea Salis: Conceptualization (lead); Funding Acquisition (equal); Supervision (equal); Writing-Review &Editing (equal).

Maura Monduzzi: Funding Acquisition (equal); Supervision (equal); Visualisation (lead); Writing – Original Draft Preparation; Writing-Review & Editing (equal).

Declaration of interests

The authors declare that they have no known competing financial interests or personal relationships that could have appeared to influence the work reported in this paper.

Highlights

- ESI/MS technique provides information on protein-electrolyte interaction
- Electrolytes added to BSA in denaturing condition induce fragmentation of BSA
- NaCl stabilizes BSA ionized interface against hydolysis and fragmentation at acid pH
- Bromide anion induces the highest extent of BSA fragmentation
- New specific electrolyte perturbation parameters quantify Hofmeister effects